Feasibility of a wave logger for freshwater nearshore applications

Amanda L. Caskenette, Andrea Kneale, Sarah Glowa, Eva C. Enders

Fisheries and Oceans Canada
Ecosystems and Oceans Science
Ontario and Prairie Region
Freshwater Institute
Winnipeg, MB
R3T 2N6

2020

Canadian Technical Report of Fisheries and Aquatic Sciences 3397

Fisheries and Oceans Canada | Pêches et Océans Canada

Canada

Canadian Technical Report of Fisheries and Aquatic Sciences

Technical reports contain scientific and technical information that contributes to existing knowledge but which is not normally appropriate for primary literature. Technical reports are directed primarily toward a worldwide audience and have an international distribution. No restriction is placed on subject matter and the series reflects the broad interests and policies of Fisheries and Oceans Canada, namely, fisheries and aquatic sciences.

Technical reports may be cited as full publications. The correct citation appears above the abstract of each report. Each report is abstracted in the data base *Aquatic Sciences and Fisheries Abstracts*.

Technical reports are produced regionally but are numbered nationally. Requests for individual reports will be filled by the issuing establishment listed on the front cover and title page.

Numbers 1-456 in this series were issued as Technical Reports of the Fisheries Research Board of Canada. Numbers 457-714 were issued as Department of the Environment, Fisheries and Marine Service, Research and Development Directorate Technical Reports. Numbers 715-924 were issued as Department of Fisheries and Environment, Fisheries and Marine Service Technical Reports. The current series name was changed with report number 925.

Rapport technique canadien des sciences halieutiques et aquatiques

Les rapports techniques contiennent des renseignements scientifiques et techniques qui constituent une contribution aux connaissances actuelles, mais qui ne sont pas normalement appropriés pour la publication dans un journal scientifique. Les rapports techniques sont destinés essentiellement à un public international et ils sont distribués à cet échelon. II n'y a aucune restriction quant au sujet; de fait, la série reflète la vaste gamme des intérêts et des politiques de Pêches et Océans Canada, c'est-à-dire les sciences halieutiques et aquatiques.

Les rapports techniques peuvent être cités comme des publications à part entière. Le titre exact figure au-dessus du résumé de chaque rapport. Les rapports techniques sont résumés dans la base de données *Résumés des sciences aquatiques et halieutiques.*

Les rapports techniques sont produits à l'échelon régional, mais numérotés à l'échelon national. Les demandes de rapports seront satisfaites par l'établissement auteur dont le nom figure sur la couverture et la page du titre.

Les numéros 1 à 456 de cette série ont été publiés à titre de Rapports techniques de l'Office des recherches sur les pêcheries du Canada. Les numéros 457 à 714 sont parus à titre de Rapports techniques de la Direction générale de la recherche et du développement, Service des pêches et de la mer, ministère de l'Environnement. Les numéros 715 à 924 ont été publiés à titre de Rapports techniques du Service des pêches et de la mer, ministère des Pêches et de l'Environnement. Le nom actuel de la série a été établi lors de la parution du numéro 925.

Canadian Technical Report of
Fisheries and Aquatic Sciences 3397

2020

FEASIBILITY OF A WAVE LOGGER FOR FRESHWATER NEARSHORE APPLICATIONS

by

Amanda Caskenette, Andrea Kneale, Sarah Glowa, and Eva C. Enders

Fisheries and Oceans Canada
Ecosystems and Oceans Science
Ontario and Prairie Region
Freshwater Institute
Winnipeg, MB
R3T 2N6

Cat. No. Fs97-6/3397E-PDF ISBN 978-0-660-35884-0 ISSN 1488-5379

Correct citation for this publication:
Caskenette, A.L., Kneale, A., Glowa, S., and Enders, E.C. 2020. Feasibility of a wave logger for freshwater nearshore applications. Can. Tech. Rep. Fish. Aquat. Sci. 3397: vii + 27 p.

.

TABLE OF CONTENTS

TABLE OF CONTENTS iii
LIST OF TABLES iv
LIST OF FIGURES v
ABSTRACT vi
RÉSUMÉ vi
ACKNOWLEDGEMENTS vii
1.0 STUDY RATIONALE 8
2.0 WAVE LOGGER DEVELOPMENT AND CALIBRATION 8
2.1 Device Specifications 8
2.2 Principles of Operation 10
2.3 Device Calibration 10
3.0 TEST SITE SPECIFICATION 11
4.0 WAVE LOGGER DEPLOYMENT 12
5.0 DATA ANALYSIS 13
5.1 Data Trimming 13
5.2 Instantaneous Angle of Displacement 13
5.3 Wave Frequency Determination 14
5.4 Statistical Analysis 14
6.0 RESULTS 15
6.1 Data ANALYSIS GuiDAnce 15
6.2.1 Wave Frequency 18
6.2.2 Instantaneous Angle of Displacement 18
7.0 DISCUSSION 23
7.1 Wave frequency 23
7.2 Instantaneous angle of displacement 25
7.3 Wave Logger Feasibility 26
References 27

LIST OF TABLES

Table 1. Data collected at Patricia Beach, Sunset Beach, and Lester Beach in Lake Winnipeg using a wave logger and a WEATHERmeter. 17

Table 2. Results of regression models for the relationship of the wave frequency to wind speed at the summer 2019 Lake Winnipeg sampling locations 20

Table 3. Results of regression models for the relationship of the 95th percentile instantaneous angle of displacement (*IAD*) to wind speed (*WS*) at the summer 2019 Lake Winnipeg sampling locations. 21

Table 4. Results of regression models for the relationship of the mean instantaneous angle of displacement (*IAD*) to wind speed (*WS*) at the summer 2019 Lake Winnipeg sampling locations. 22

LIST OF FIGURES

Figure 1. Wave logger set-up. A HOBO® Pendant G data logger is attached to the top of a float, created from ABS pipe, that is attached to a 4.5 kg anchor with a rigid tether on a swivel. 9

Figure 2. Map and graphical description of test sites in the south basin of Lake Winnipeg, Manitoba, Canada. Large arrows indicate the point of access to the sites, green areas represent shoreline vegetation, gray circles represent boulders, and the spaces within the boxes represent the transects. 12

Figure 3. Wave logger output when converted to instantaneous angle of displacement. The original output (a) was corrected for the calibration angle (b), angle when device is at rest, to obtain the true instantaneous angle of displacement (c). A single wave (d) was counted at the peak (e). The mean instantaneous angle of displacement (f) and the 95th percentile (g) were used in the analyses. 14

Figure 4. Raw wave logger data at Lester Beach on August 26, 2019 (round 4). Dotted lines indicate the time of deployment and retrieval determined from the analysis of the acceleration in the z-axis. Data points recorded pre- and post-deployment were removed from further analysis. 15

Figure 5. Initial 920 s of raw and true instantaneous angle of displacement calculated from trimmed wave logger data collected at Lester Beach on August 26, 2019 (round 4). 16

Figure 6. Wave frequency and wind speed data collected from the initial hour of nine record periods at the summer 2019 Lake Winnipeg sampling locations. 18

Figure 7. Mixed linear model with fixed intercept and random slope relationship between 95th percentile instantaneous angle of displacement (*IAD*) and wind speed (*WS*) calculated from initial hour of eight record periods at the summer 2019 Lake Winnipeg sampling for four different wind conditions, i.e., wind from east-northeast direction (ENE), no wind (none), south-southwest direction (SSW), and west-southwest direction (WSW). 19

Figure 8. Mixed linear model with fixed intercept relationship between wind speed (*WS*) and mean instantaneous angle of displacement (*IAD*) calculated from initial hour of nine record periods at the summer 2019 Lake Winnipeg sampling locations for four different wind conditions, i.e., wind from east-northeast direction (ENE), no wind (none), south-southwest direction (SSW), and west-southwest direction (WSW). 19

Figure 9. Initial 20 s of trimmed wave logger data converted to calibrated instantaneous angle of displacement at Patricia Beach on September 16, 2019 (round 5). 24

Figure 10. Initial 20 s of trimmed wave logger data converted to calibrated instantaneous angle of displacement at Lester Beach on August 26, 2019 (round 4). 24

ABSTRACT

Caskenette, A.L., Kneale, A., Glowa, S., and Enders, E.C. 2020. Feasibility of a wave logger for freshwater nearshore applications. Can. Tech. Rep. Fish. Aquat. Sci. 3397: vii + 27 p.

Wave action generates a wide variety of nearshore physical processes that contribute to acute behavioural and structural changes of nearshore ecosystems. Wave action is difficult to measure however, and most available devices are either expensive or inappropriate for short term deployments in shallow waters. A wave logger designed for shallow water use was deployed in Lake Winnipeg, Canada for five rounds at three sites to examine the ability of the wave logger to appropriately represent underwater forces. There was no relationship between wind speed and wave frequency. There was a significant positive relationship between wind speed and the 95% and mean instantaneous angle of displacement (*IAD*), which is a measure of force, dependent on site and wind direction. Deployments with a faster recording rate are needed to determine if the device can be used to measure wave frequency. The wave logger was useful when measuring the magnitude of underwater forces created by the waves and thus, there is potential for this device to quantify the role wave action plays in structuring nearshore communities.

RÉSUMÉ

Caskenette, A.L., Kneale, A., Glowa, S., and Enders, E.C. 2020. Feasibility of a wave logger for freshwater nearshore applications. Can. Tech. Rep. Fish. Aquat. Sci. 3397: vii + 27 p.

L’action des vagues génère une grande variété de processus physiques littoraux qui contribuent aux changements comportementaux et structurels aigus des écosystèmes côtières. L’action des vagues est cependant difficile à mesurer et la plupart des dispositifs disponibles sont soit chers, soit inappropriés pour des déploiements à court terme dans des eaux peu profondes. Un enregistreur de vagues conçu pour une utilisation en eau peu profonde a été déployé dans le lac Winnipeg, Canada, pendant cinq campagne de terrain sur trois sites afin d’examiner la capacité de l’enregistreur de vagues à représenter correctement les forces sous-marines. Il n’y avait aucune relation entre la vitesse du vent et la fréquence des vagues. Il y avait une relation positive significative entre la vitesse du vent et les 95% et l’angle de déplacement instantané moyen (*ADI*), qui est une mesure de la force, en fonction du site et de la direction du vent. Des déploiements avec une fréquence d'enregistrement plus rapide sont nécessaires pour déterminer si l’appareil peut être utilisé pour mesurer la fréquence des ondes. L’enregistreur de vagues a été utile pour mesurer l’ampleur des forces sous-marines créées par les vagues et, par conséquent, il existe un potentiel pour ce dispositif pour quantifier le rôle joué par l’action des vagues dans la structuration des communautés côtières.

ACKNOWLEDGEMENTS

Fisheries and Oceans Canada (DFO) wishes to acknowledge the contributions of those in the Riverine Ecology Lab who collected field data for the technical report. Financial support for this project was provided by the Fisheries and Oceans Canada's (DFO) Aquatic Invasive Species Monitoring Program and the Manitoba Fish and Wildlife Enhancement Fund.

1.0 STUDY RATIONALE

Waves affect the structure and function of the entire water column in nearshore ecosystems (Seibt et al. 2013). Energy from waves cause undercurrents, displace organisms from substrates, cause movement and mixing of fine sediments, and deliver nutrients and plankton from offshore ecosystems. These factors contribute to patterns of fish abundance and community composition and can have a chronic effect at a site, affecting populations over time (Probst et al. 2009; Stoll et al. 2010). Similarly, the effects of wave energy may contribute to acute behavioural and structural changes of the nearshore community at the time of data collection.

Due to the importance of wave forces on the nearshore community, it is important to consider waves when analysing data collected in the nearshore environment. If wave forces are not considered when examining nearshore community dynamics, then changes to nearshore communities due to wave forces may be misattributed. However, most devices available to study waves are either expensive or inappropriate for short term deployments in shallow waters (Figurski et al. 2011). To determine the wave action in the frame of the Nearshore Sampling Program in Lake Winnipeg that aims to determine the effect of the recent invasion and ongoing expansion of Zebra Mussels (*Dreissena polymorpha*) in Lake Winnipeg on the structure and function of the nearshore community, a wave logger was developed. This wave logger was modelled after the URSKI (Figurski et al. 2011) and deployed in the summer of 2019. This report discusses the development and deployment of the wave logger and analyzes preliminary data to determine the feasibility of the device for future research.

Two key factors that contribute to the frequency of waves and the underwater forces enacted by waves are: (1) wind and (2) shoreline topography (Schutten et al. 2004). If relationships between these factors and wave frequency and force can be determined, then it may not be necessary to measure wave frequency and force directly. Conversely, site specific differences may contribute considerably to wave frequency and underwater forces, requiring direct measurements of wave frequency and force.

In summary, the objectives of this report are to describe: 1) wave logger development and calibration, 2) wave logger deployment, 3) data analysis, and 4) to discuss the feasibility of the wave logger for use in freshwater nearshore environments.

2.0 WAVE LOGGER DEVELOPMENT AND CALIBRATION

2.1 DEVICE SPECIFICATIONS

The wave logger was modelled after the URSKI wave logger that was created to measure wave forces in nearshore ocean environments (Figurski et al. 2011). The set-up consists

of a float, tether, anchor, and HOBO® Pendant G Acceleration Data Logger (UA-004-64, Onset, Bourne, MA, USA) that measures acceleration and angular displacement in the x-, y-, and z-axes (Figure 1). The device stands 43 cm total in height.

Figure 1. Wave logger set-up. A HOBO® Pendant G data logger is attached to the top of a float, created from ABS pipe, that is attached to a 4.5 kg anchor with a rigid tether on a swivel.

An acceleration data logger was selected because the unit is small, waterproof, inexpensive, and has sufficient accuracy (0.735 m/s^2 at 25°C) and resolution (0.245 m/s^2). The data logger records time series data that can be downloaded directly to a computer. The data logger was attached to the top of the float (Figure 1).

The float was made of black ABS pipe with a cap glued on the bottom and a threaded female adaptor hub glued to the top to fit a male plug. The air in the float provided enough buoyancy for the device to sit upright in still water. The float is capable of being opened in order to add water to reduce the amount of the air in the float, thereby reducing the buoyancy. The data logger was attached to the float using a bracket that was handmade out of an 7.5 cm piece of aluminum. This allowed for the logger to be attached perpendicular to the float. The bracket was made as small as possible to not influence the action of the water. The bracket was screwed into the float then epoxied to prevent water

entering the float. The logger was attached with a nut and bolt through a hole in the bracket. The logger was removable and adjustable.

The tether was constructed from a solid metal pole (32.5 cm in height). The pole was epoxied into the bottom cap of the float through a hole drilled in the bottom of the cap. For further stability, a nut and bolt were put through the pole and attached to the float. Epoxy was added to waterproof the float.

A 4.5 kg lead weight was used to temporarily anchor the device to the lake bottom during the sampling period. The anchor ensured that the device remained in a fixed location during the sampling period but could easily be transported between locations. A swivel bracket was epoxied into the anchor to attach the tether. The epoxy was not enough to support the stress of moving the logger between locations, therefore a modification was made for further stability. Holes were drilled around the anchor and wire was strung through the swivel and anchor. Epoxy was then applied to the swivel to keep it in place, however the tether, float and by extension, the logger, were able to move freely in all directions on the swivel bracket. A hole was then drilled into the tether pole and connected to the swivel bracket using metal wire. The anchor had an eye bolt drilled and epoxied into the side to enable another 4.5 kg lead weight to be attached with airline cable. To not interfere with the wave logger, a yellow float was attached to the second lead weight using rope to mark the logger. The second anchor was also set-up to hold additional loggers (e.g., temperature, light) if needed.

2.2 PRINCIPLES OF OPERATION

A wave logger moves with wave surge in an arc defined by the length of tether. The magnitude of the displacement of the device depends on the water velocity and the wave period, and is calculated from the proportion of gravity (g) recorded in the horizontal axes of the accelerometer. The instantaneous angle of displacement (IAD), therefore, is calculated from the magnitude of the vector sum of accelerations in the x-and y-axes:

$$IAD_i = arcsin\left(\frac{\sqrt{x_i^2 + y_i^2}}{g}\right) \quad (1)$$

where x_i and y_i are the measured accelerations for each axis at time i and g is gravity (9.8 m/s^2). A detailed description of the principles of operation for the wave logger is available in Figurski et al. (2011).

2.3 DEVICE CALIBRATION

The wave logger does not sit perfectly upright, this resulting angle at rest is defined as the calibration angle. To determine the calibration angle, the device was placed in still water

in a large tank indoors. The recorded calibration angle was then subtracted from all subsequently measured instantaneous angle of displacement (*IAD*).

3.0 TEST SITE SPECIFICATION

The wave logger was tested at three sites located on the east shore in the south basin of Lake Winnipeg (Figure 2):

- Patricia Beach (50.423570, -96.616360): Sandy beach east of Netley Marsh.
- Sunset Beach (50.496262, -96.598824): Beach lined with groynes (boulders) and sand/gravel substrate.
- Lester Beach (50.581073, -96.584610): Sandy beach with some rocks and boulders.

These sites were chosen based on the relative abundance of hard substrate (very low, low, and medium) and were sampled every three weeks over a sampling period of one to two days, randomizing what site was sampled first. The sites encompassed a rectangular area 180 m along the shoreline in length by 20 m offshore in width. Each site was broken into nine 20 m wide transects. One transect was randomly chosen as the transect for the wave measurements. The water depths at each site were variable depending on the water levels in the lake, but were consistently less than 1.25 m at 20 m from shore, and decreased as the shoreline was approached.

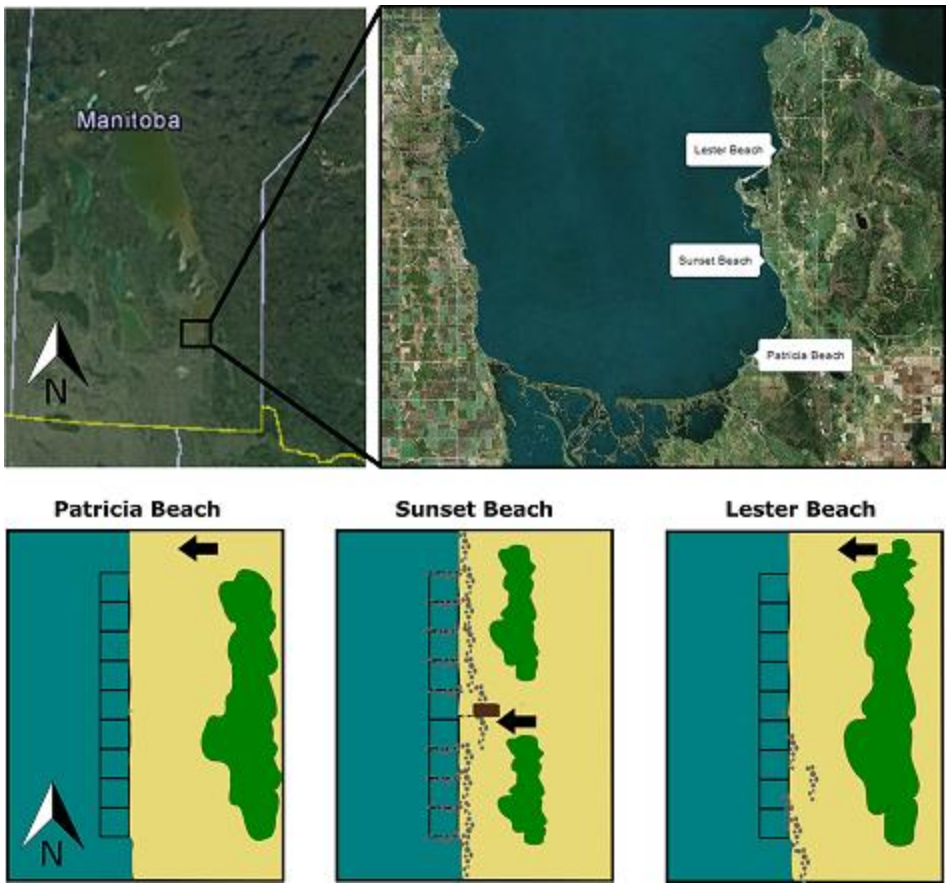

Figure 2. Map and graphical description of test sites in the south basin of Lake Winnipeg, Manitoba, Canada. Large arrows indicate the point of access to the sites, green areas represent shoreline vegetation, gray circles represent boulders, and the spaces within the boxes represent the transects.

4.0 WAVE LOGGER DEPLOYMENT

In the transect for wave measurements, the wave logger was deployed at a water depth of 63 cm resulting in the acceleration logger being 20 cm below the surface. The wave logger was left in the water for the entire time sampling occurred at the site, with a minimum soak of 1 h. The wave logger data was downloaded onto a laptop using the HOBO® Waterproof Shuttle (U-DTW-1) before leaving the site.

After the logger was deployed at each site, field staff completed three replicate counts of waves breaking on shore in 20 s. Wind direction and strength were measured at each site using a WEATHERmeter (WeatherFlow, Scotts Valley, CA, USA). A WEATHERmeter is a miniature weather station connected to a smartphone application via Bluetooth that collects real-time wind, temperature, humidity, and pressure readings. The weather variables including wind speed were only measured once, when the crew first arrived at the site.

The wave logger was deployed on four to five separate occasions at three sites (Patricia Beach, Sunset Beach, and Lester Beach, Figure 2) for a total of twelve record periods. The acceleration data logger installed on the wave logger was set to record acceleration in the x-, y-, and z-axes at a frequency of 1 Hz during the deployment period. The waterproof shuttle attached to a laptop was used onshore to initialize the recording prior to deploying the wave logger, and the data recording was manually stopped once the wave logger was back onshore.

5.0 DATA ANALYSIS

5.1 DATA TRIMMING

Data at the beginning and end of the data record, that was not part of the deployment period, needed to be trimmed in a consistent way. The acceleration in the z-axis remained fairly constant when the logger was deployed with a mean standard deviation of 0.06 g, while pre- and post-deployment values had a broader range. This observation was used to trim the data by removing all values prior to and following the period when the acceleration readings were fairly constant in the z-axis. A data record was considered to be part of the deployment period if the average of 25 consecutive z-acceleration values was equal to the mean of the z-acceleration values in the middle of the time series. In addition, the first 200 values in this period were removed to ensure that only values from the logging period were included.

5.2 INSTANTANEOUS ANGLE OF DISPLACEMENT

The instantaneous angle of displacement (*IAD*) of the wave logger was used as a relative measure of wave force (Figurski et al. 2011). For each record period the *IAD* was calculated from the magnitude of the vector sum of accelerations in the horizontal x- and y-axes recorded by the acceleration data logger at each 1 s record (Eq. 1). The vector sum of the x- and y-axes was outside of the arcsin domain (−1 to +1) during 2 rounds at each site (six record periods in total) contributing to 0.01–3% of the data per record period. These data were ignored for this analysis, but further analyses are needed to determine the cause of these erroneous values. The calibration angle measured in the laboratory (Figure 3b) was subtracted from the *IAD* calculated from the field data (Figure 3a) to calculate the true *IAD* (Figure 3c).

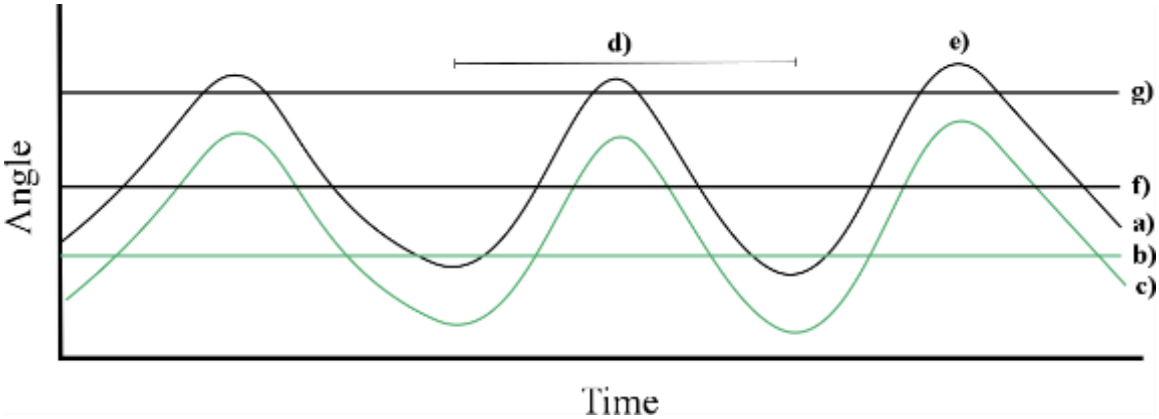

Figure 3. Wave logger output when converted to instantaneous angle of displacement. The original output (a) was corrected for the calibration angle (b), angle when device is at rest, to obtain the true instantaneous angle of displacement (c). A single wave (d) was counted at the peak (e). The mean instantaneous angle of displacement (f) and the 95th percentile (g) were used in the analyses.

5.3 WAVE FREQUENCY DETERMINATION

The peak of a single wave (Figure 3e) was determined if the *IAD* for a single record was greater than the *IAD* preceding or following the measurement. If the preceding *IAD* was greater than the *IAD* in question, then the wave was considered to be falling; as in the peak of that wave had already occurred. If the following *IAD* was greater than the *IAD* in question then the wave was considered to be rising but not yet at the peak.

The total number of waves calculated to occur during the first hour was divided by 20 seconds (s) to determine the 20 s wave frequency. The 20 s wave frequency was compared to the mean in-situ field record of three replicate counts of waves breaking on shore in 20 s.

5.4 STATISTICAL ANALYSIS

Wave frequency and *IAD* should increase with increasing wind speed. To determine if the interpretation of the data from the devices was as expected we performed statistical analyses of the relationship between the wave logger data and wind speed.

The wave frequency, and 95th percentile and mean *IAD* calculated from the first hour of sampling were compared to wind speed using regression models to determine if wind speed could explain the variation in the wave frequency and/or *IAD*. Site and wind direction were included as categorical variables to determine if they affected the relationship between wind speed and the response variables. Distribution fitting was completed for the wave frequency and 95th percentile and mean *IAD* data to select probability distributions that best fit the data. The best fit probability distributions were used to determine the regression equations, coefficient of determination (r^2), and significance values (p). The site labels were included on the graphs to visually evaluate if the data was clustered by site. Akaike information criterion (AIC) was used to assess the

quality of each model relative to the other models. All statistical analyses were performed in R (RStudio Team 2019).

6.0 RESULTS

6.1 DATA ANALYSIS GUIDANCE

As an example of the data recorded from the acceleration data logger during a given record period, the raw data retrieved from a wave logger installed at Lester Beach on August 26, 2019 (round 4) is presented (Figure 4).

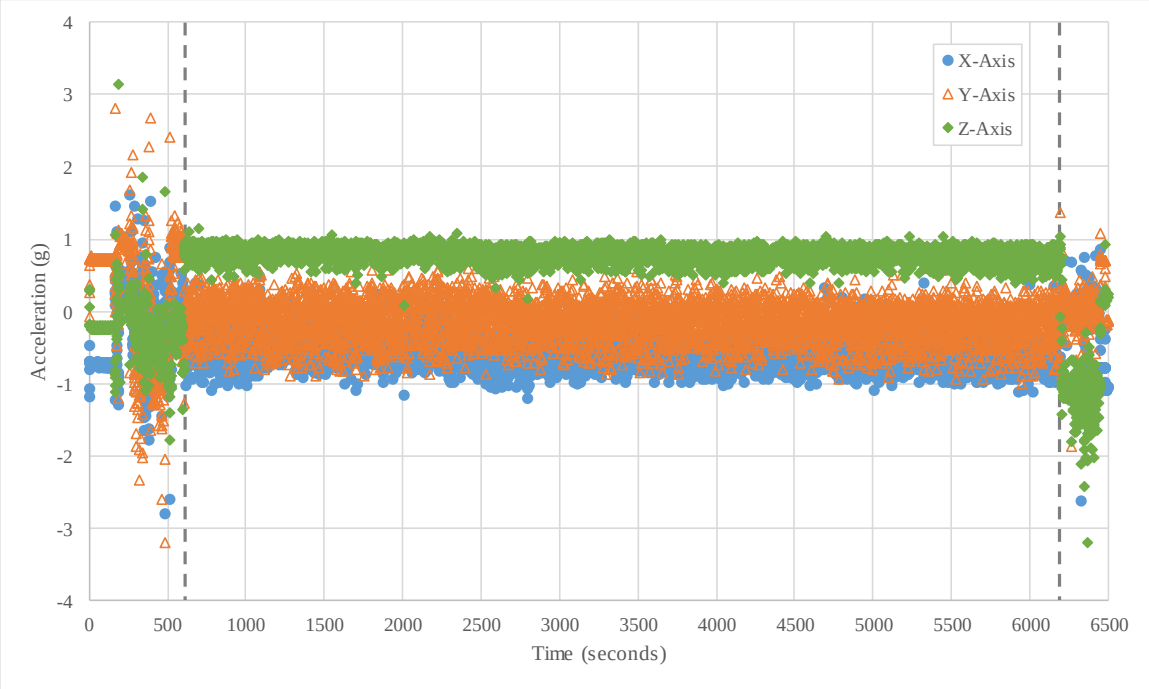

Figure 4. Raw wave logger data at Lester Beach on August 26, 2019 (round 4). Dotted lines indicate the time of deployment and retrieval determined from the analysis of the acceleration in the z-axis. Data points recorded pre- and post-deployment were removed from further analysis.

The initial 920 s of raw and true *IAD* data calculated from trimmed wave logger data collected at Lester Beach on August 26, 2019 (round 4) is presented (Figure 5). The true *IAD* was calculated by subtracting the calibration angle from the raw *IAD* calculated from the field data. Negative true *IAD* values indicate that the wave logger rotated past the resting (calibration) angle as a result of the wave force. The true *IAD* values were used to analyze the efficacy of the wave logger.

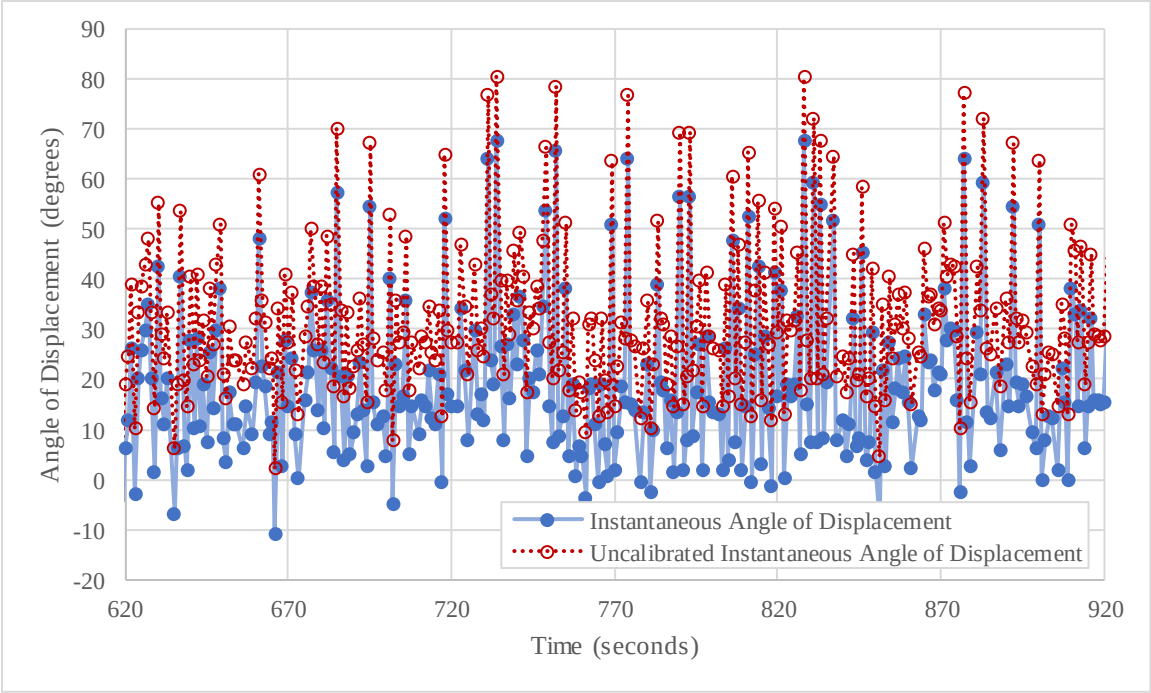

Figure 5. Initial 920 s of raw and true instantaneous angle of displacement calculated from trimmed wave logger data collected at Lester Beach on August 26, 2019 (round 4).

The wave frequency and maximum, 95th percentile, and mean *IAD* values calculated from the first hour of wave logger sampling, as well as the mean in-situ field record of three replicate counts of waves breaking on shore in 20 s, wind speed, wind gust, and wind direction data at the 2019 wave logger field sites are presented (Table 1). The deployment periods ranged from approximately 1 h 20 m (Patricia Beach round 4) to 4 h 20 m (Sunset Beach round 2). Only the initial hour of the deployment periods minus the first 200 records was used for analysis to maintain consistency between sites and rounds (total of 56 m and 40 s). The first 200 s of the deployment period were removed to ensure no pre-deployment records were included in the analysis. The wind speed ranged from 0 m s^{-1} (Patricia Beach round 3 and Sunset Beach round 3) to 11 m s^{-1} (Sunset Beach round 5). The highest maximum *IAD* was 77° at Lester Beach round 3 (wind 6.1 m s^{-1}) and Sunset Beach round 5 (wind 11 m s^{-1}). The highest 95th percentile and mean *IAD* was 57° and 32° at Lester Beach round 3 (wind 6.1 m s^{-1}), followed by 52° and 26° at Lester Beach round 4 (wind 7.7 m s^{-1}).

Wave frequency calculated from the wave logger data ranged from five to eight waves per 20 s, with the peak wave frequency calculated at Lester Beach round 2 (wind 1.1 m s^{-1}). Wave frequency as counted in-situ ranged from six to 20 waves per 20 s, with the peak wave frequency recorded at Patricia Beach round 5 (wind 3.5 m s^{-1}).

Table 1. Data collected at Patricia Beach, Sunset Beach, and Lester Beach in Lake Winnipeg using a wave logger and a WEATHERmeter.

Site	Round	Date	Total Time Period of Round	Maximum Instantaneous Angle of Displacement (°)	95th Percentile Instantaneous Angle of Displacement (°)	Mean Instantaneous Angle of Displacement (°)	Total No. of Waves	20-Second Wave Frequency	Mean Manual Count of Waves in 20 Seconds	Wind Speed (m s^{-1})	Wind Gust (m s^{-1})	Wind Direction
Lester Beach	R2	16-Jul-19	2:02:51	19	5.7	0.0015	1290	7.6	12	1.1	2.2	WSW
	R3	9-Aug-19	2:47:17	77	57	32	929	5.5	7	6.1	7.4	WSW
	R4	26-Aug-19	1:33:00	75	52	27	1039	6.1	8	7.7	9.8	WSW
	R5	16-Sep-19	4:01:56	13	7.5	4.0	1129	6.6	10	5	7.5	ENE
Patricia Beach	R2	16-Jul-19	1:59:20	62	13	0.55	1203	7.1	10	0.9	2.2	WSW
	R3	9-Aug-19	1:58:12	39	18	3.5	1303	7.7	11	0	0	None
	R4	25-Aug-19	1:22:00	40	17	3.1	1188	7.1	11	3.7	4.7	WSW
	R5	16-Sep-19	2:14:12	26	7.4	2.9	1067	6.3	20	3.5	8.1	ENE
Sunset Beach	R2	16-Jul-19	4:22:53	16	6.1	0.52	1218	7.2	13	1.4	2.3	WSW
	R3	9-Aug-19	2:38:10	8.2	4.7	2.2	959	5.6	6	0	0	None
	R4	26-Aug-19	2:33:00	49	20	5.1	1261	7.4	10	4.3	6.2	WSW
	R5	18-Sep-19	2:25:22	77	45	16	1127	6.6	9	11.1	17.4	SSW

Notes:
- the calibration angle for the wave logger was 13°
- all wave logger data is calculated from the initial 56 min and 40 s of sampling

6.2.1 Wave Frequency

The wave frequency data follows a normal probability distribution. There was no relationship between wave frequency and wind speed (r^2 = 0.04, p = 0.26) (Figure 6). The majority of 20 s wave frequencies recorded by the wave logger did not equal the in-situ field record of three replicate counts of waves breaking on shore in 20 s (Table 1). Site and wind direction did not affect the wave frequency – wind speed relationship (**Table 2**).

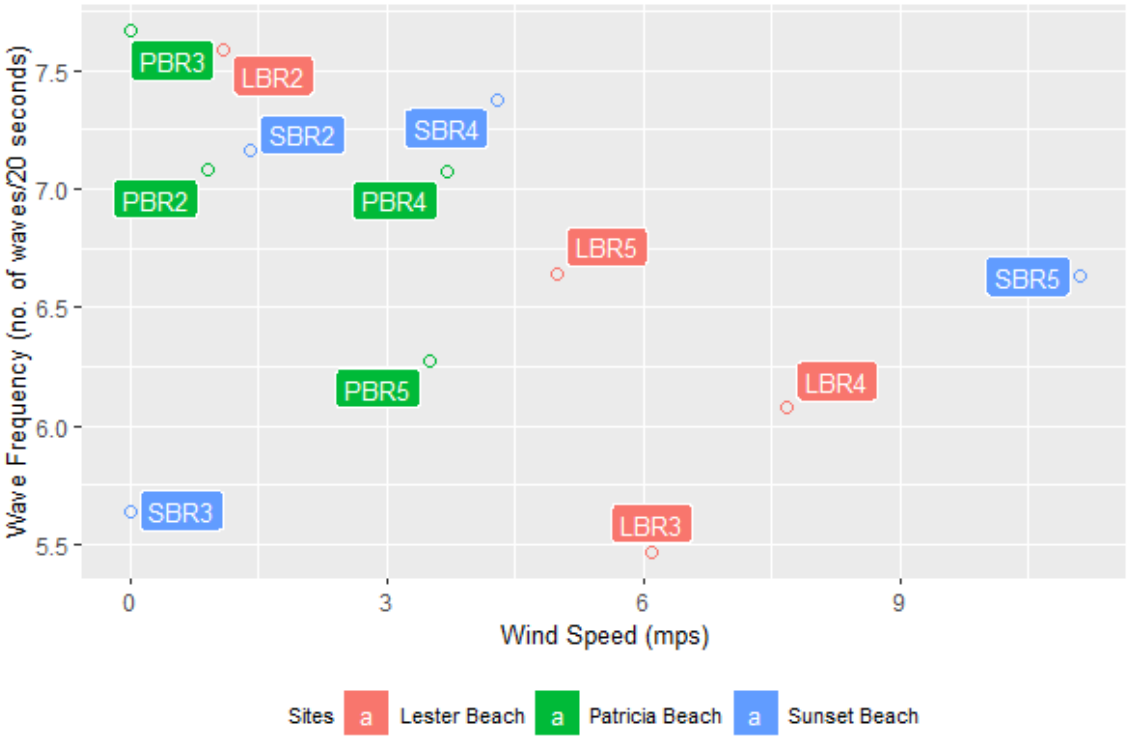

Figure 6. Wave frequency and wind speed data collected from the initial hour of nine record periods at the summer 2019 Lake Winnipeg sampling locations.

6.2.2 Instantaneous Angle of Displacement

The 95th and mean *IAD* data follow log-normal probability distributions. Four regression models were analyzed using the 95th and mean *IAD* data in relation to wind speed to determine goodness-of-fit (**Table 3** and **Table 4**). The fixed effect of site and/or wind direction on the data was included in the multiple linear regression models. The adjusted r^2 increased and the AIC decreased with the inclusion of site and wind direction indicating that site and wind direction are factors in the relationship between wind speed and *IAD*. There is a positive relationship between wind speed and the 95th percentile (r^2 = 0.808, p = 0.016) and mean *IAD* (r^2 = 0.694, p = 0.046) recorded during the initial hour of the deployment period (Figure 7 and Figure 8).

Figure 7. Mixed linear model with fixed intercept and random slope relationship between 95th percentile instantaneous angle of displacement (*IAD*) and wind speed (*WS*) calculated from initial hour of eight record periods at the summer 2019 Lake Winnipeg sampling for four different wind conditions, i.e., wind from east-northeast direction (ENE), no wind (none), south-southwest direction (SSW), and west-southwest direction (WSW).

Figure 8. Mixed linear model with fixed intercept relationship between wind speed (*WS*) and mean instantaneous angle of displacement (*IAD*) calculated from initial hour of nine record periods at the summer 2019 Lake Winnipeg sampling locations for four different wind conditions, i.e., wind from east-northeast direction (ENE), no wind (none), south-southwest direction (SSW), and west-southwest direction (WSW).

Table 2. Results of regression models for the relationship of the wave frequency to wind speed at the summer 2019 Lake Winnipeg sampling locations

Predictors	Linear			Linear with fixed effect of site			Linear with fixed effect of wind direction			Linear with fixed effect of site and wind direction		
	Estimates	Std. Error	p	Estimates	Std. Error	p	Estimates	Std. Error	p	Estimates	Std. Error	p
a	7.01	0.32	**<0.001**	6.73	0.54	**<0.001**	7.36	0.70	**<0.001**	7.19	1.04	**0.001**
b	-0.08	0.06	0.257	-0.06	0.08	0.464	-0.21	0.11	0.098	-0.20	0.15	0.238
$c_{site,PB}$				0.41	0.59	0.510				0.22	0.71	0.763
$c_{site,SB}$				0.22	0.55	0.708				-0.10	0.76	0.901
$c_{ws,none}$							-0.71	0.87	0.441	-0.60	1.03	0.585
$c_{ws,SSW}$							1.63	1.17	0.208	1.74	1.66	0.341
$c_{ws,WSW}$							0.23	0.59	0.704	0.32	0.70	0.669
Observations	12			12			12			12		
r^2 / r^2 adjusted	0.126 / 0.039			0.175 / -0.134			0.370 / 0.009			0.400 / -0.319		
p	0.2572			0.6519			0.4563			0.7525		
AIC	29.896			33.200			31.978			35.379		

Notes:
- *WF* = wave frequency
- *WS* = wind speed
- regression equation: $\log(WF) = a + b \cdot WS + c_{ws,none} + c_{ws,SSW} + c_{ws,WSW} + c_{site,PB} + c_{site,SB}$

Table 3. Results of regression models for the relationship of the 95th percentile instantaneous angle of displacement (*IAD*) to wind speed (*WS*) at the summer 2019 Lake Winnipeg sampling locations.

Predictors	Linear			Linear with fixed effect of site			Linear with fixed effect of wind direction			Linear with fixed effect of site and wind direction		
	Estimates	Std. Error	p	Estimates	Std. Error	p	Estimates	Std. Error	p	Estimates	Std. Error	p
a	1.96	0.28	**<0.001**	1.88	0.47	**0.004**	0.68	0.48	0.204	0.28	0.49	0.588
b	0.19	0.06	**0.007**	0.21	0.07	**0.012**	0.31	0.08	**0.005**	0.35	0.07	**0.004**
$c_{site,PB}$				0.27	0.51	0.618				0.52	0.33	0.173
$c_{site,SB}$				-0.23	0.48	0.650				-0.25	0.35	0.514
$c_{ws,none}$							1.55	0.60	**0.037**	1.81	0.48	**0.013**
$c_{ws,SSW}$							-0.34	0.81	0.686	-0.05	0.77	0.949
$c_{ws,WSW}$							1.05	0.41	**0.037**	1.25	0.33	**0.012**
Observations	12			12			12			12		
R^2 / R^2 adjusted	0.535 / 0.489			0.586 / 0.431			0.797 / 0.682			0.913 / 0.808		
p	**0.006847**			0.05904			**0.01419**			**0.01553**		
AIC	27.131			29.742			23.168			17.042		

Notes:
- *IAD* = instantaneous angle of displacement
- *WS* = wind speed
- regression equation: $\log(IAD) = a + b \cdot WS + c_{ws,none} + c_{ws,SSW} + c_{ws,WSW} + c_{site,PB} + c_{site,SB}$

Table 4. Results of regression models for the relationship of the mean instantaneous angle of displacement (*IAD*) to wind speed (*WS*) at the summer 2019 Lake Winnipeg sampling locations.

Predictors	Linear			Linear with fixed effect of site			Linear with fixed effect of wind direction			Linear with fixed effect of site and wind direction		
	Estimates	Std. Error	p	Estimates	Std. Error	p	Estimates	Std. Error	p	Estimates	Std. Error	p
a	-0.94	0.99	0.365	-2.28	1.63	0.199	-3.02	1.88	0.153	-6.14	1.81	**0.019**
b	0.45	0.2	**0.047**	0.54	0.23	**0.045**	1.00	0.30	**0.012**	1.35	0.26	**0.003**
$c_{site,PB}$				1.91	1.79	0.318				3.23	1.23	**0.046**
$c_{site,SB}$				1.15	1.67	0.511				2.96	1.32	0.074
$c_{ws,none}$							4.03	2.34	0.129	4.05	1.78	0.072
$c_{ws,SSW}$							-5.28	3.16	0.139	-9.06	2.87	**0.025**
$c_{ws,WSW}$							-0.33	1.59	0.841	-0.25	1.22	0.843
Observations	12			12			12			12		
r^2 / r^2 adjusted	0.339 / 0.273			0.423 / 0.206			0.647 / 0.446			0.861 / 0.694		
p	**0.04709**			0.1997			0.08512			**0.04609**		
AIC	57.311			59.681			55.771			48.598		

Notes:
- *IAD* = instantaneous angle of displacement.
- *WS* = wind speed
- regression equation: $\log(IAD) = a + b \cdot WS + c_{ws,none} + c_{ws,SSW} + c_{ws,WSW} + c_{site,PB} + c_{site,SB}$

7.0 DISCUSSION

A wave logger was developed to measure the underwater forces of waves in the nearshore environment. This report outlines the development and deployment of the logger and examines the ability of the logger to appropriately represent the underwater forces. We compared the wave logger output to wind measurements, with the prediction that wave frequency and forces would be positively related to wind speed.

7.1 WAVE FREQUENCY

Contrary to expectations, there was an insignificant negative relationship between the frequency of waves and wind speed. This was most likely due to the inability to properly identify wave frequency.

The presented method to determine wave frequency, as well as the record frequency of the acceleration logger, may result in erroneous wave counts. For example, since the acceleration logger is set to record data at 10 Hz, that resulted in ten measurements every second, high wave frequencies may cause misidentification of rising and falling sections of waves as peaks. In the method used, a peak must be preceded and followed by a lower instantaneous angle of displacement, and the low recording frequency may miss these parts of the wave, or when the peak was hit. The in-situ field records of three replicate counts of waves breaking on shore in 20 s indicate that, in some instances, the analysis of the wave logger data likely undercounted the number of waves during deployment (Table 1). For example, Figure 9 and Figure 10 present the initial 20 s of trimmed wave logger data converted to calibrated instantaneous angle, and wave peaks as determined by this method. The wave peaks indicated by the red box equal one wave count. Therefore during the time period depicted in Figure 9 six waves occurred in the first 20 s of deployment and in Figure 10 six were counted, however the wind speed and manual count were comparatively much higher. It is unclear if the wave peaks are all a result of new waves or are part of the rising and falling limbs of a wave. In future wave logger trials, the acceleration logger should be set-up to record data in fast mode for a higher frequency of measurements (up to once every 0.01 s). Increasing the record frequency will decrease the duration of data collection that can be recorded due to increased battery usage, but with short deployments this should not be an issue.

Counting erratic measurements in the rising and falling limbs of a wave as a wave peak may result in an erroneously high number of waves during deployment. If the float of the wave logger isn’t buoyant enough, the wave logger may respond erratically to the force from a single wave. Additional trials should be completed with a larger float to determine the effects of the buoyancy of the float on the instantaneous angle of displacement.

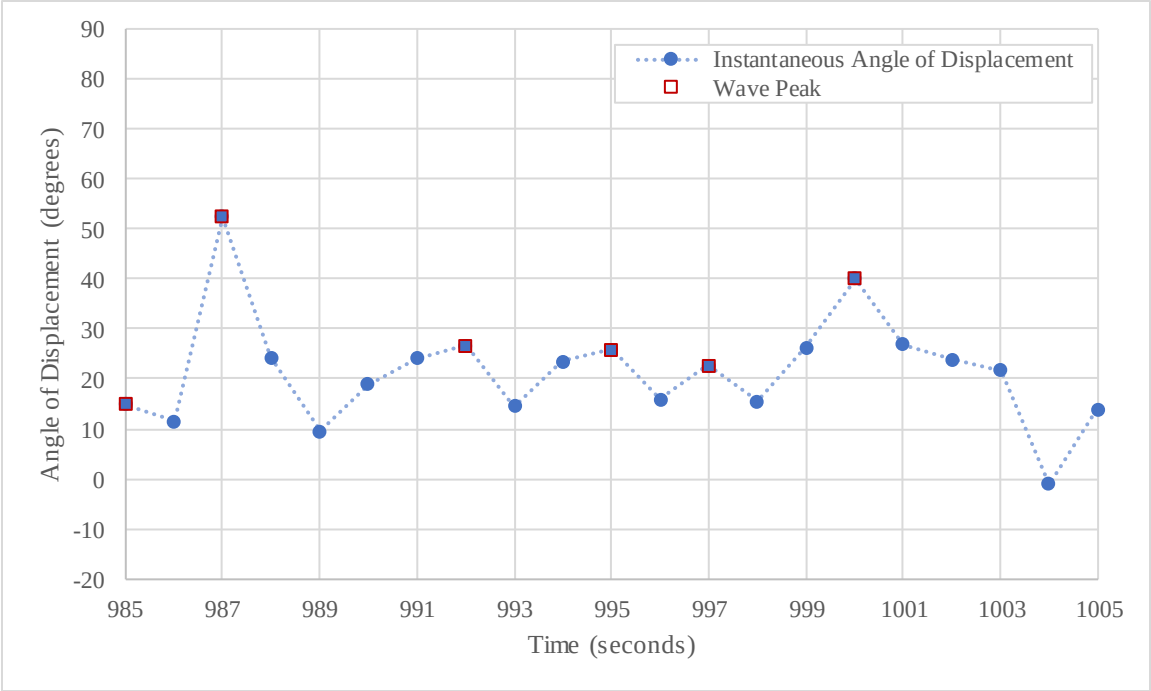

Figure 9. Initial 20 s of trimmed wave logger data converted to calibrated instantaneous angle of displacement at Patricia Beach on September 16, 2019 (round 5).

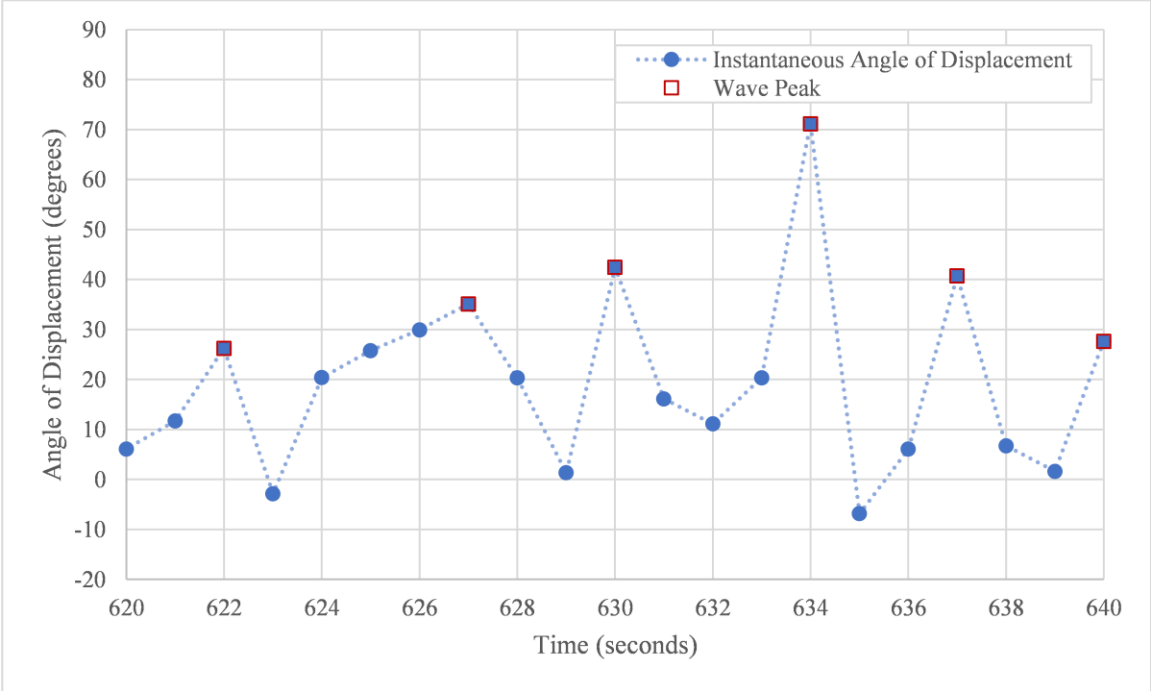

Figure 10. Initial 20 s of trimmed wave logger data converted to calibrated instantaneous angle of displacement at Lester Beach on August 26, 2019 (round 4).

When there was a measurable wind, the wind direction was west-southwest for most sites and rounds except for Patricia Beach round 5 (wind direction = east-northeast) and

Sunset Beach round 5 (wind direction = south-southwest), which were the only rounds logged in September. The wind direction would affect the position of the waves relative to the shore and therefore should affect wave frequency. Wind direction was not included in the best model of the relationship between frequency of waves and wind speed. This was more likely due to not adequately measuring wave frequency, rather than evidence of a lack of effect of wind direction. The lack of fit between the wave frequency and the wind speed may also have been due to wind speed or direction changing during the sampling period, or due to a lag in the response of the wave frequency to wind speed and direction changes. In future wave logger trials, the wind speed and direction should be recorded at regular intervals throughout, and prior to the deployment period.

Our approach to counting wave peaks was quite simplistic. Many equations exist, including that of a regular sinusoidal wave, to approximate the characteristics of a wave (Craig et al. 2006). In reality, waves are complex and non-linear, with a random mix of small and large waves, and the underwater forces caused by waves, which we are measuring here, are even more complicated with other fluid motions coming into play (St. Laurent et al. 2012). Deploying the wave loggers with a higher recording frequency may enable us to determine the appropriate equation to describe the dynamics of underwater movement in the nearshore. Trials in a controlled environment would allow for a better understanding of the underwater dynamics of the wave logger and the wave frequency.

The design that this wave logger was modelled after (URSKI, Figurski et al. 2011) was only used to measure wave force, not wave frequency. This may be due to the authors encountering similar issues in the field. It is also possible that it was beyond the scope of the analyses they envisioned for the device.

7.2 INSTANTANEOUS ANGLE OF DISPLACEMENT

The underwater force exerted by a wave in the nearshore environment increased with increasing wind speed. There was a positive relationship between both the mean and 95th percentile *IAD* and wind speed, and the best models according to AIC included site and wind direction.

Contrary to wave frequency, the relative force exerted by the underwater currents associated with the waves can be directly calculated from the acceleration data. A more detailed description of how the acceleration is converted to an angle which represents relative force is provided in Figurski et al. (2011). The upper 95% quantile of *IAD* is useful when determining the greatest amount of force the community would have encountered during the sampling period, while avoiding spurious data. There was a large range of maximum forces within a site between rounds, and between sites. By directly measuring these forces, rather than estimating based on wind or visual approximation, these differences can be accounted for in the analyses of the biological data collected.

Importantly, these differences in wave forces can also be accounted for in the analysis of nutrients and detritus in the water column, denoting when they were likely to be suspended by wave forces in the water column.

In addition, we calculated the mean *IAD*, the interpretation of what this represents is a little more complicated. When the device is hit by a wave, it first tilts with the force of the wave (positive displacement) and then returns upright when the wave has past, sometimes moving past the upright position in the opposite direction (negative displacement). If the next wave hits the logger before it returns to the upright position, then the mean *IAD* would be greater than if it were to return to upright position, and greater than if there was negative displacement. Larger forces would cause a greater positive displacement, increasing the amount of time it would take for the device to return to the upright position. Therefore, the mean *IAD* may represent a combination of wave frequency and wave force. Further analysis, with a greater recording frequency, would be needed to determine if this is the case.

Wind direction and site were included in the best model. The direction of the wind will affect the fetch and subsequently wave height and the wave angle at which the waves encounter the shore and may complicate the underwater currents. The site specific structure of the beach likely affects the underwater currents. While all three sites were on the east shore of the south basin of Lake Winnipeg, there were differences in the topography and composition of substrates (Figure 2). Patricia Beach consisted of large sandbars whose location changed during the course of the year. Lester Beach consisted mainly of sand, but the south end of the beach included some cobble and boulders. The transects at Sunset Beach were separated by groynes, also known as wave breaks. All of these factors would affect the underwater forces exerted by the waves. These site and direction specific differences in underwater forces would not be accounted for if only wind speed or waves breaking on shore were measured as a proxy for underwater forces caused by the waves.

7.3 WAVE LOGGER FEASIBILITY

The wave logger appeared to work as designed to determine the force of the waves in the nearshore environment, and is a better measure than wind speed alone due to the differences between sites and wind directions. We do not, however, feel that we have been able to determine if this device can accurately measure wave frequency. More trials are needed with a higher recording frequency for both the wave logger and for measurements of wind speed. The interpretation of the wave logger data would also benefit from trials performed in a controlled environment like an indoor wave chamber with known wave properties.

REFERENCES

Craig, W., Guyenne, P.; Hammack, J., Henderson, D., and Sulem, C. 2006. Solitary water wave interactions, Physics of Fluids, 18 (57106): 057106–057106–25, doi:10.1063/1.2205916

Figurski, J.D., Malone, D., Lacy, J.R., and Denny, M. 2011. An inexpensive instrument for measuring wave exposure and water velocity: Measuring wave exposure inexpensively. Limnol. Oceanogr. Methods 9(5): 204–214. doi:10.4319/lom.2011.9.204

Probst, W.N., Stoll, S., Hofmann, H., Fischer, P., and Eckmann, R. 2009. Spawning site selection by Eurasian perch (*Perca fluviatilis* L.) in relation to temperature and wave exposure. Ecol. Freshw. Fish 18(1): 1–7. doi:10.1111/j.1600-0633.2008.00327.x

Seibt, C., Peeters, F., Graf, M., Sprenger, M., and Hofmann, H. 2013. Modeling wind waves and wave exposure of nearshore zones in medium-sized lakes. Limnol. Oceanogr. 58(1): 23–36. doi:10.4319/lo.2013.58.1.0023

Schutten, J., Dainty, J., Davy, J. 2004. Wave-induced Hydraulic Forces on Submerged Aquatic Plants in Shallow Lakes. Annals of Botany. 93(3): 333-341. doi:10.1093/aob/mch043

Stoll, S., Hofmann, H., and Fischer, P. 2010. Effect of wave exposure dynamics on gut content mass and growth of young-of-the-year fishes in the littoral zone of lakes. J. Fish Biol. 76(7): 1714–1728. doi:10.1111/j.1095-8649.2010.02611.x

St. Laurent, L. Alford, M.H., and Paluszkiewicz, T. 2012 An introduction to the special issue on internal waves. Oceanography, 25 (2): 15–19. doi:www.jstor.org/stable/24861339